Assessment of the paleoseismic potential of the Ferrum site along the southernmost San Andreas fault using new UAV imagery, GPR data, and preliminary trenching

William C. Buckley[1], Thomas K. Rockwell[1], Katherine M. Scharer[2], Allen M. Gontz[3], Paula M. Figueiredo[4], & Zoe A. Morgan[1]

[1]San Diego State University; [2]United States Geological Survey-CA; [3]Clarkson University; [4]North Carolina State University

Abstract

We initiated studies along the southern San Andreas fault at Ferrum, CA, where a double releasing bend has ponded Holocene alluvium against an uphill-facing scarp. Ferrum is located along the east side of the Salton Sea between Bombay Beach and North Shore, about 2 km north of Salt Creek. We constructed high-resolution orthomosaics and digital surface models (DSMs) generated from Structure-from-Motion-Multiview Stereo (SfM-MVS) techniques from uncrewed aerial vehicle (UAV) imagery. The images, along with field mapping, were used to identify and measure fault-related offsets of geomorphic features that have been preserved through the past two to three inundations of ancient Lake Cahuilla. The most recent event appears to have produced between 2 and 3.5 m of lateral slip, with lower overall lateral slip values where multiple strands are present. We also identify offset channels with up to ~7 meters of lateral deflection, which are interpreted as representing multiple (probably 2) events. A cluster of small-scale offsets was identified, generally with displacements of less than a meter but a few up to ~1.5 meters, which probably reflect displacement from creep that postdate the most recent lake and large earthquake event. Along with the UAV imagery interpretations, we acquired ground penetrating radar (GPR) data to map the upper several meters of the subsurface architecture of the fault zone and ponded alluvial sediment to examine stratigraphy and locate faults and fault-related deformation. Following the geophysical analysis, we excavated two 1.5-2 m deep trenches to collect samples for radiocarbon dating to constrain ages on shallow sediments, identify and date lake events, and to verify findings from the GPR surveys. The trenches revealed excellent stratigraphy and evidence for preservation of lake deposits from the most recent lake event (Lake A), along with several minor fault splays. The primary fault is located beneath thick dune deposits. We collected over 50 radiocarbon samples, all gastropod shells, representing nearly all stratigraphic units exposed in the trench walls to develop the site chronology and assess the site's potential for dating earthquake events.

Study Site

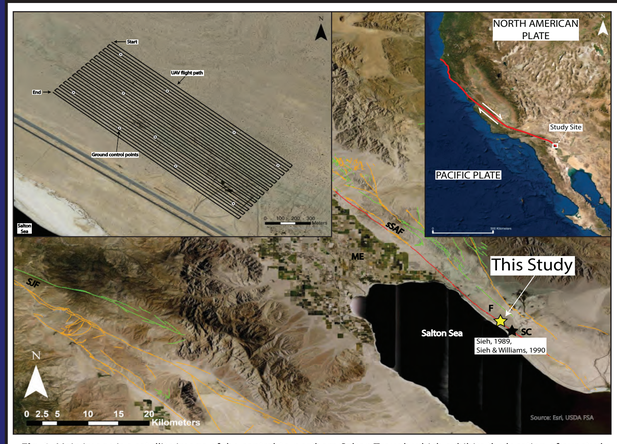

Fig. 1. Main image is a satellite image of the central-to-northern Salton Trough which exhibits the location of our study site (in Ferrum, CA) near the modern-day Salton Sea shoreline, the regional Quaternary faults (USGS and CGS, 2021), and a nearby paleoseismic study at Salt Creek. Inset figure (upper left) displays our UAV flight path with start and end points, along with Ground Control Point (GCP) locations which were used to construct decimeter-scale orthomosaics and hillshade maps from UAV imagery. Inset figure (upper right) shows a map of North America in relation to our study site with the location of the San Andreas Fault (SAF) between the boundary of the North American and Pacific Plates. Abbreviations: sSAF - southernmost San Andreas Fault, SJF - San Jacinto Fault, ME - Mecca, F - Ferrum, SC - Salt Creek.

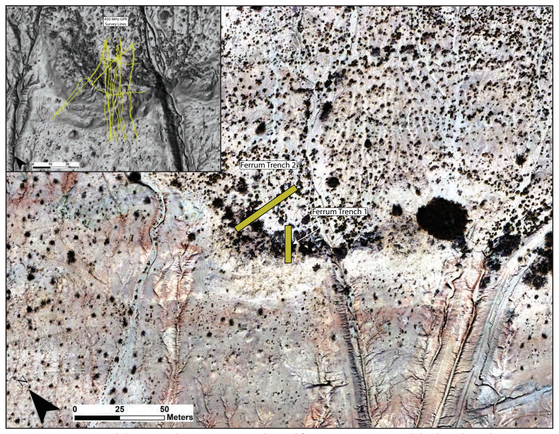

Fig. 2. Main image exhibits an orthomosaic image derived from UAV imagery and displays the paleoseismic trenches from our study. Ferrum Trench 1 provided the best stratigraphic record with evidence for one lake event (Lake A) and revealed several minor fault splays. Detailed trench logs are available for Ferrum Trench 1; see Figs. 10 and 11. Inset figure (upper left) exhibits a hillshade map derived from UAV imagery with a GPR track map (yellow lines) overlain from a GPR survey we conducted with a 450MHz antennae. GPR profiles revealed minor faulting that was verified with trenching.

Fig. 3. (right) A DJI Phantom Pro 4 UAV system was used for our UAV survey of the study area. UAV imagery was collected during one field day and was later processed using Agisoft Metashape to create decimeter-scale orthomosaics and DSMs. The DSMs were exported to ArcGIS to create various maps such as hillshade and topographic maps in order to analyze the geomorphic context of fault-related features at our study site and to identify the location of trenching.

Fig. 4. (right) Field photo taken during our GPR survey. A Mala Ground Explorer (GX) GPR system with a 450MHz antennae was used prior to trenching to acquire a map of the subsurface environment, analyze the stratigraphy, and locate faults to facilitate the location of paleoseismic trenches. Detailed GPR profiles are available for two of the survey lines that run parallel to Ferrum Trench 1 (see Figs. 13 and 14).

Reconstructions

Hillshades

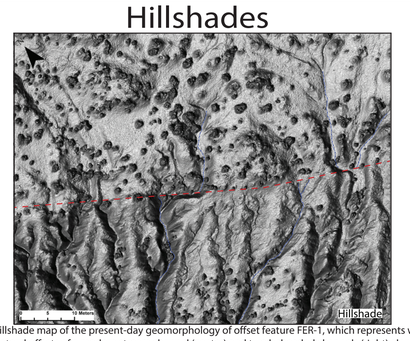

Fig. 5a. Hillshade map of the present-day geomorphology of offset feature FER-1, which represents well-preserved lateral offsets of a modern stream channel (center) and two beheaded channels (right) along the main trace of the sSAF in Ferrum. Fault trace and channel thalwegs are depicted by red and blue dashed lines, respectively.

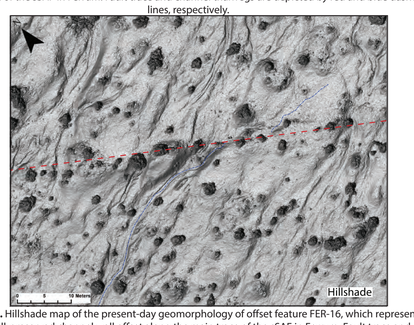

Fig. 5b. Hillshade map of the present-day geomorphology of offset feature FER-16, which represents a well-preserved channel wall offset along the main trace of the sSAF in Ferrum. Fault trace and channel thalwegs are depicted by red and blue dashed lines, respectively.

Best-fit

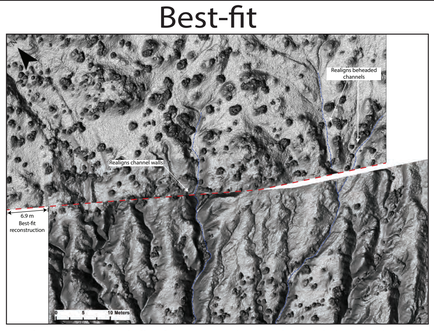

Fig. 6a. Best-fit reconstruction of offset feature FER-1 showing channel thalwegs realigned to original configuration before offset occurred. Realignment measures 6.9 m of lateral offset, suggesting that these features have been preserved through the last two (2) large earthquake events.

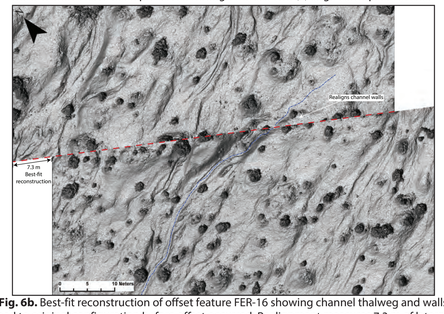

Fig. 6b. Best-fit reconstruction of offset feature FER-16 showing channel thalweg and walls realigned to original configuration before offset occurred. Realignment measures 7.3 m of lateral offset, suggesting that this feature has been preserved through the last two (2) large earthquake events.

Minimum

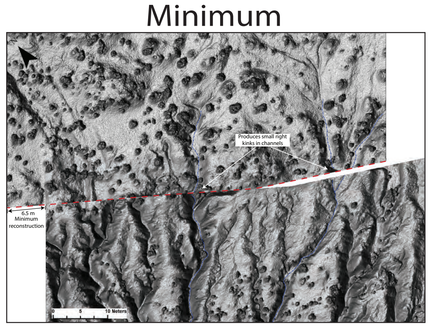

Fig. 7a. Minimum reconstruction of offset feature FER-1 showing channel thalwegs realigned in a way that produces a small right kink in channels. Minimum realignment measures 6.5 m of lateral offset, providing a -0.4 m uncertainty for our best-fit reconstruction.

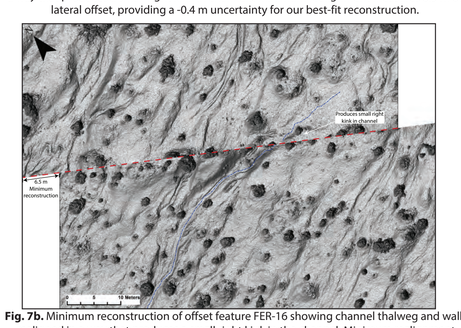

Fig. 7b. Minimum reconstruction of offset feature FER-16 showing channel thalweg and walls realigned in a way that produces a small right kink in the channel. Minimum realignment measures 6.5 m of lateral offset, providing a -0.8 m uncertainty for our best-fit reconstruction.

Maximum

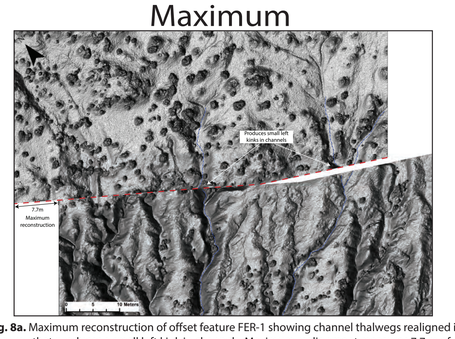

Fig. 8a. Maximum reconstruction of offset feature FER-1 showing channel thalwegs realigned in a way that produces a small left kink in channels. Maximum realignment measures 7.7 m of lateral offset, providing a +0.8 m uncertainty for our best-fit reconstruction.

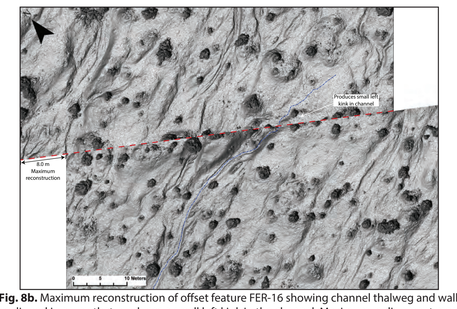

Fig. 8b. Maximum reconstruction of offset feature FER-16 showing channel thalweg and walls realigned in a way that produces a small left kink in the channel. Maximum realignment measures 8.0 m of lateral offset, providing a +0.7 m uncertainty for our best-fit reconstruction.

Topo Maps

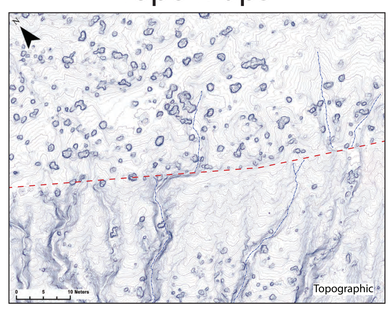

Fig. 9a. Topographic map of the present-day topography offset feature FER-1. Contours were generated using ArcGIS Pro with 10 cm contour intervals.

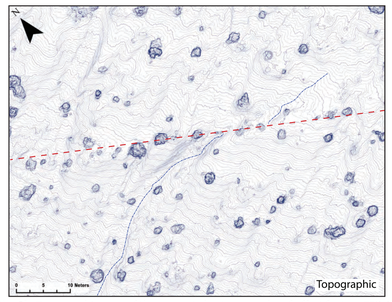

Fig. 9b. Topographic map of the present-day topography of offset feature FER-16. Contours were generated using ArcGIS Pro with 10 cm contour intervals.

Trench Logs

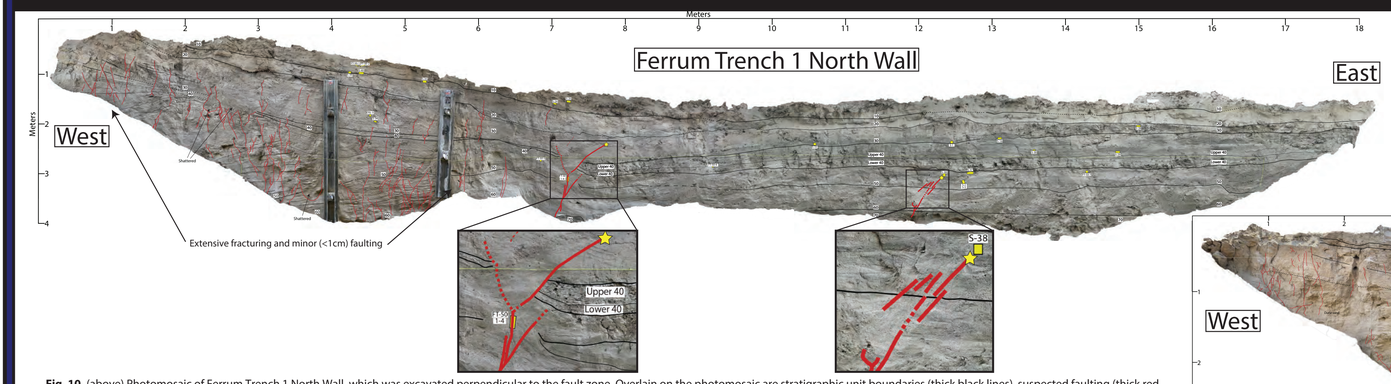

Fig. 10. (above) Photomosaic of Ferrum Trench 1 North Wall, which was excavated perpendicular to the fault zone. Overlain on the photomosaic are stratigraphic unit boundaries (thick black lines), suspected faulting (thick red lines), fracturing (thin red lines), and sample locations for C14 and OSL dating. Extensive fracturing was observed along the west end of the trench, coincident to where thick deposits of dune sand were observed. Minor faulting was observed at approximately 7.5 and 12.5 m from the west end of the trench and event horizons have been noted (yellow stars), although the absence of similar faulting on south wall complicates interpretation of these deformation features. The main fault zone is suspected to be located just beyond the west end of the trench, below the thick dune deposits. Inset figures exhibit fault-related deformation.

Fig. 11. (below) Photomosaic of Ferrum Trench 1 South Wall (reflected), which was excavated perpendicular to the fault zone. Overlain on the photomosaic are stratigraphic unit boundaries (thick black lines), fracturing (thin red lines), and sample locations for C14 and OSL dating. Extensive fracturing was observed along the west end of the trench, coincident to where thick deposits of dune sand were observed. The main fault zone is suspected to be located just beyond the west end of the trench, below the thick dune deposits.

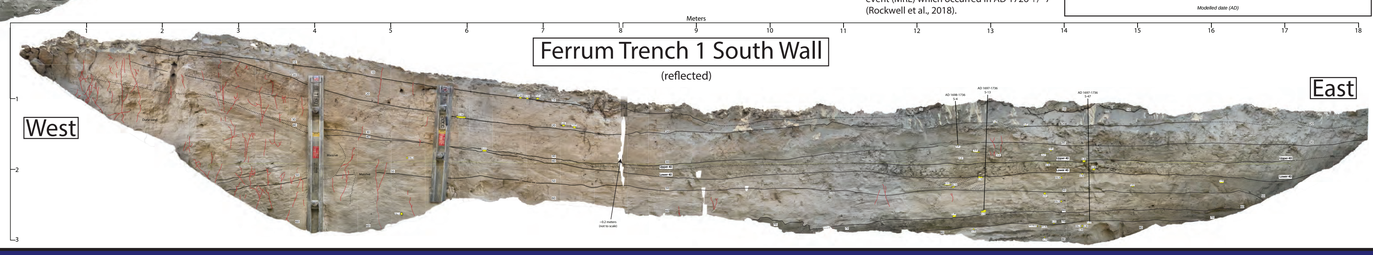

Fig. 12. (right) Radiocarbon (C14) analysis was performed at the Keck Carbon Cycle AMS Facility at UC Irvine on 35 gastropod samples collected from Ferrum Trench 1. Most samples appeared to have been reworked, with modeled ages that appeared to be much older than what we suspect. Three of the samples (S-4, S-13, and S-47), which are located in upper and lower units of Ferrum Trench 1 South Wall, appeared to have minimal reworking and provided modeled ages dating between AD 1697 and 1736. These three samples provide evidence that the minor faulting observed in Ferrum Trench 1 represents that of the most recent event (MRE) which occurred in AD 1726 +/- 7 (Rockwell et al., 2018).

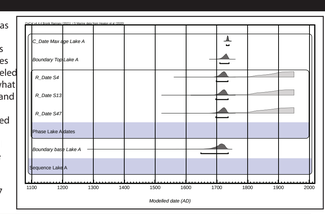

GPR Profiles

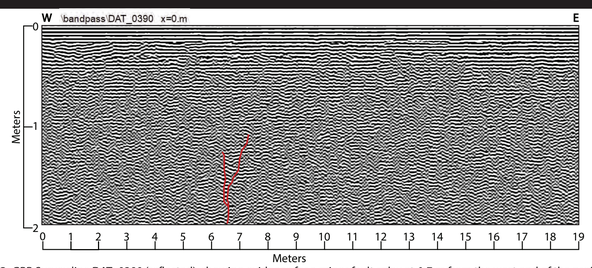

Fig. 13. GPR Survey line DAT_0390 (reflected), showing evidence for a minor fault splay at 6-7 m from the west end of the profile. DAT_0390 ran directly over the location of Ferrum Trench 1 and is reflected to match the west and east ends of the trench.

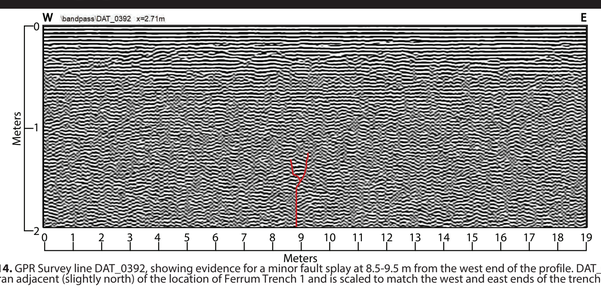

Fig. 14. GPR Survey line DAT_0392, showing evidence for a minor fault splay at 8.5-9.5 m from the west end of the profile. DAT_0392 ran adjacent (slightly north) of the location of Ferrum Trench 1 and is scaled to match the west and east ends of the trench.

Discussion

- DSMs from this study reveal several well-preserved geomorphic features with lateral offsets ranging up to ~7.3 m from our best-fit reconstruc-tions, suggesting that these features have been preserved through the last two (2) major earthquake events.
- Paleoseismic trenching revealed excellent stratigraphy, several minor fault splays, and provided an abundance of gastropods which facilitated sampling that represented nearly all stratigraphic units exposed in the trench walls.
- C14 analysis suggests that the Holocene deposits observed in our paleoseismic trenching originated from the most recent lake event (Lake A), dating between AD 1697 and 1736.
- GPR surveys exhibited evidence for a minor fault splay that was co-located with a minor fault splay observed in Ferrum Trench 1; however, an abundance of highly conductive materials such as salt, gypsum, and clay in the subsurface at our study site made any stratigraphic interpreta-tions under ~0.5 m difficult.
- Future work will be performed at this site to better understand the faulting mechanisms and tectonic framework in the area and will, in part, consist of implementing additional geophysical surveys such as Electrical Resistivity Tomography (ERT) and Seismic Reflection to better capture the subsurface environment.
- Important note: main author will be present via Zoom for questions/explanations Mon-Wed during SCEC event from approximately 3-3:30pm.